Heliyon 8 (2022) e09975

Contents lists available at ScienceDirect

Heliyon

journal homepage: www.cell.com/heliyon

Research article

Atmospheric aerosol particle size distribution from Lidar data based on the lognormal distribution mode

Yuchen Shi [a,b], Wenqing Liu [b], Yunsheng Dong [b,*], Xuesong Zhao [b], Yan Xiang [b], Tianshu Zhang [b], Lihui Lv [b]

[a] University of Science and Technology of China, School of Environmental Science and Optoelectronic Technology, 96 Jinzhai Road, Hefei, Anhui, CN, 230000, China
[b] Hefei Institutes of Physical Science, Anhui Institute of Optics and Fine Mechanics, ChuangXin Avenue, LuYang District, Hefei, Anhui, CN, 230000, China

ARTICLE INFO

Keywords:
APSD
Lognormal particle size distribution
6S
Lidar

ABSTRACT

Analysis of the atmospheric Aerosol Particle Size Distribution (APSD) retrieved from Light Detection and Ranging (Lidar) data is one of the popular fields in atmospheric remote sensing. An APSD retrieval method based on the lognormal particle size distribution, the Mie theory, and the Second Simulation of the Satellite Signal in the Solar Spectrum (6S) were studied. According to the 6S, this method divides the main body of the aerosols into four basic components and calculates the APSD from Lidar data and the optical and microphysical characteristics of these components. Numerical simulation and experimental observations reveal that this method can obtain the APSD for particle sizes of >0.15 μm in the different vertical layers with good reliability.

1. Introduction

Atmospheric aerosols are one of the main causes of air pollution and have had a great impact on climate change and the social economy (Ding et al., 2009). Comprehensive and accurate calculation of the Aerosol Particle Size Distribution (APSD) in polluted areas can help to analyze the sources and causes of air pollution. This knowledge could lead to a great improvement in the control of atmospheric aerosols, haze, and other air pollution components. The direct APSD measuring methods include light-scattering, aerodynamic, and piezoelectric crystal (Mao et al., 2002). These methods have high accuracy but can only obtain data near the observation station. A solar photometer can effectively measure the APSD by obtaining the aerosol optical depth at different wavelengths from the information about solar radiation (Yang et al., 2008). However, a solar photometer cannot retrieve the APSD in the different vertical layers, and high spatial resolution Light Detection and Ranging (Lidar) data could fill the gap in this research field.

As a new atmospheric APSD observation instrument, multi-wavelength Lidar has high temporal and spatial resolutions. The principle of measuring the APSD is to observe and retrieve the optical characteristics at different wavelengths, such as the backscattering coefficients and extinction coefficients, and match the optical characteristics with the microphysical characteristics using different methods to calculate the atmospheric APSD. In 1999, Müller proposed a method based on the Fredholm integral equations to obtain optical data related to the physical quantities. This algorithm uses inversion with regularization to retrieve the physical parameters of the tropospheric particle size distribution (Müller et al., 1999a, 1999b). In 2000, Müller observed the APSD using Lidar data from the Aerosol Characterization Experiment 2 (ACE 2) and the Lindenberg Aerosol Characterization Experiment 98 (LACE 98). The retrieved APSDs were compared with the results obtained using other related devices and found to be in good agreement with the direct measuring results (Müller et al., 2000). From 2018 to 2019, professor Hua and his team used the Fredholm algorithm to retrieve the APSDs in Xi'an and optimized the process based on the local meteorological conditions (Rao et al., 2018; Di et al., 2019; Yan et al., 2019). These studies provide effective cases for the application of this algorithm.

The Fredholm algorithm has high retrieval accuracy and spatial resolution, and it is not dependent on historical data or atmospheric models (Müller et al., 1999a, 1999b). However, the effective retrieved results rely on the sensitive response of the backscattering coefficients and the extinction coefficients to the APSD at specific wavelengths, so the algorithm has high requirements for the emission and reception wavelengths of the Lidar system. In this study, we developed a method based on the Second Simulation of the Satellite Signal in the Solar Spectrum (6S) and the lognormal particle size distribution. The proposed method was verified through numerical simulations to demonstrate that it can be used with Lidar data retrieval, and the Pearson correlation coefficient between

* Corresponding author.
E-mail address: ysdong@aiofm.ac.cn (Y. Dong).

https://doi.org/10.1016/j.heliyon.2022.e09975
Received 9 March 2022; Received in revised form 25 April 2022; Accepted 13 July 2022

the raw data and the retrieved results was found to be >0.95. Relying on the model data, this method has lower requirements for the Lidar system compared with the Fredholm algorithm, and the parameters can be adjusted according to the observation location and the local meteorological conditions to improve the retrieval accuracy.

2. Inversion principle

The principle of the method is to match the Lidar-data-retrieved extinction coefficients with the model-calculated coefficients to obtain information about the atmospheric aerosol components and to obtain the APSD results. The method can be separated into three main steps: obtaining the extinction coefficients based on Lidar data; matching the theoretical extinction coefficients calculated using Mie theory and 6S with the Lidar results to obtain the aerosol component proportions; and calculating the APSD from the component proportions.

2.1. Inversion of Lidar data

The Lidar data were inverted using the Fernald algorithm (Fernald, 1984). The basic equation is

$$P(Z) = ECZ^{-2}\beta(Z)\exp\left\{-2\int_0^Z \sigma(z)dz\right\}, \quad (1)$$

where Z is the height, P(Z) is the backward signal received by the detector, E is the energy emitted by the laser pulse, C is the constant number of the Lidar system, β is the backscattering coefficient, and σ is the extinction coefficient.

The Fernald algorithm divides the main body of the atmospheric influences on the laser signals into two parts: gas molecules (subscript 1) and aerosol particles (subscript 2). The basic equation (Eq. (1)) is transformed into

$$\beta_1(Z)+\beta_2(Z) = \frac{X(Z)\exp\left[-2(S_1-S_2)\int_{Z_c}^{Z}\beta_2(z)dz\right]}{\frac{X(Z_c)}{\beta_1(Z_c)+\beta_2(Z_c)} - 2S_1\int_{Z_c}^{Z}X(z)\exp[-2(S_1-S_2)\int_{Z_c}^{z}\beta_2(z')dz']dz}, \quad (2)$$

where X(Z) is the range correction signal, S_1 is the ratio of the extinction coefficient to the backscattering coefficient of the gas molecules, and S_2 is the ratio of the aerosol particles (also called the Lidar ratio). The algorithm sets a reference height at which the atmosphere is very clean, and the aerosol part can be estimated using the U.S. standard atmosphere and the Rayleigh extinction mode (U. NOAA and U. A. Force, 1976). As such, when the algorithm is used to retrieve the aerosol extinction coefficient, the Lidar ratio S_2 is usually determined through empirical estimation or mode determination.

2.2. APSD inversion model

The particle size distribution is an important physical parameter for atmospheric aerosols. Generally, the APSD refers to the number of particles per unit volume at the logarithmic radius interval. It can be expressed by Eq. (3),

$$n(r) = \frac{dN(r)}{d\log r}, \quad (3)$$

where N(r) is the total concentration of aerosol particles with radii of less than r.

In 1997, Vermote introduced a new scattering inversion method based on Simulation of the Satellite Signal in the Solar Spectrum (5S) and proposed 6S, which is widely used in the field of atmospheric radiative transport and aerosol properties (Tanre et al., 1986; Vermote et al., 1997). The 6S simplifies the calculation of the atmospheric transport equations and interprets the atmospheric transport model and atmospheric component parameters in detail. According to the 6S, atmospheric aerosols can be divided into four typical basic components: dust-like, oceanic, water-soluble, and soot particles. The total atmospheric extinction coefficients can be calculated by summing the coefficients of the four basic components at different wavelengths, and they can also be retrieved from Lidar data using Eq. (2). Moreover, the extinction coefficients and particle size distribution of the different component proportion combinations can be calculated using Mie theory and 6S. Therefore, the APSD can be obtained by matching the Lidar date results with the 6S extinction coefficients to acquire the proportions of the aerosol components. The inversion problem can be translated into the following equation:

$$Ext^{Lidar} = Ext^{6S} = n_1Ext_1^{6S} + n_2Ext_2^{6S} + n_3Ext_3^{6S} + n_4Ext_4^{6S}, \quad (4)$$

where Ext^{Lidar} is the Lidar-data-retrieved extinction coefficient. Ext^{6S} is the total extinction coefficient calculated using 6S and is the weighted accumulation of the extinction coefficients of the four components, and n_1 to n_4 are the proportions of the four components. Eq. (4) is suitable for all of the received wavelength signals of Lidar, i.e., every wavelength can be used in Eq. (5).

$$\begin{cases} Ext^{Lidar}(\lambda_1) = n_1Ext_1^{6S}(\lambda_1) + n_2Ext_2^{6S}(\lambda_1) + n_3Ext_3^{6S}(\lambda_1) + n_4Ext_4^{6S}(\lambda_1) \\ Ext^{Lidar}(\lambda_2) = n_1Ext_1^{6S}(\lambda_2) + n_2Ext_2^{6S}(\lambda_2) + n_3Ext_3^{6S}(\lambda_2) + n_4Ext_4^{6S}(\lambda_2) \\ Ext^{Lidar}(\lambda_3) = n_1Ext_1^{6S}(\lambda_3) + n_2Ext_2^{6S}(\lambda_3) + n_3Ext_3^{6S}(\lambda_3) + n_4Ext_4^{6S}(\lambda_3) \\ \cdots\cdots \end{cases} \quad (5)$$

The extinction coefficients of every single aerosol component (Ext_i^{6S}) are calculated using Mie theory, and the input parameters include the particle size distribution, which is the solution of the method. To solve this problem, the look-up table method is used to obtain the aerosol component proportions closest to the Lidar data, i.e., to calculate the extinction coefficient values of all of the proportion combinations and create a combinations-extinction table. Then, the Lidar retrieved extinction coefficient values are matched with the table using the least squares method to determine the suitable proportion combination for the calculation of the APSD. This process is illustrated in Figure 1.

Then, the APSD can be calculated using the lognormal particle size distribution with the microphysical characteristics of the aerosol components described in the 6S.

2.3. Lognormal particle size distribution of a single component in the 6S

The lognormal particle size distribution of a single component in the 6S is shown in Eq. (6),

$$\frac{dN}{d\log r} = \frac{N}{\sqrt{2\pi}\log\sigma}\exp\left[-\frac{(\log r-\log r_m)^2}{2(\log\sigma)^2}\right], \quad (6)$$

where N is the total concentration of the aerosol particles with radii of less than r, r is the particle radius, r_m is the geometric mean radius, and σ is the geometric standard deviation. The two parameters of the lognormal function, r_m and σ, are different for the four components, and their values are shown in Table 1. In addition, the lognormal particle size distributions of the four components are shown in Figure 2.

The APSD under different atmospheric conditions can be simulated using the variations in the proportions of the four basic components. For each component, the 6S introduces two quantities, i.e., the parametric mean particle volume V_j (m^3) and the particle number concentration N_j (particle number/cm^3), to match the volume proportion with the number proportion. The values of these variables are presented in Table 2, and the relationship between these two quantities is expressed by Eq. (7),

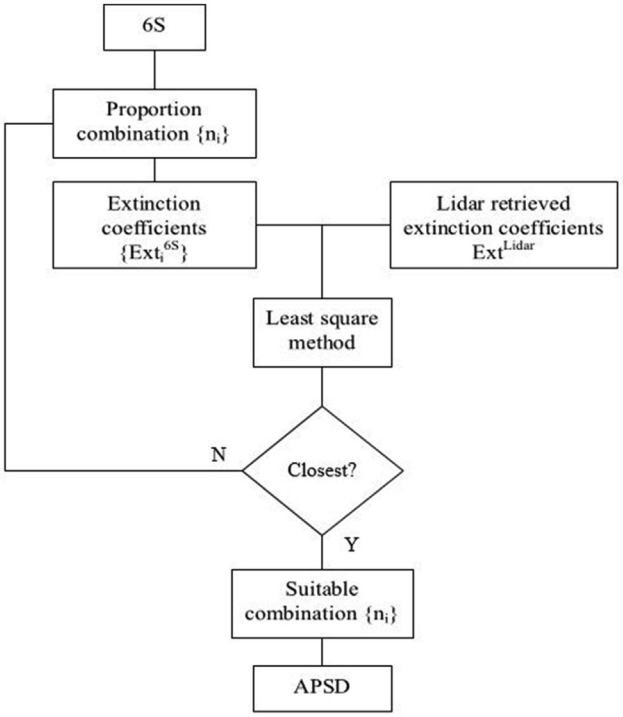

Figure 1. Process of APSD retrieval method.

Table 1. r_m and σ values for the four components.

Component	r_m (μm)	σ
Dust-like	0.500	2.99
Oceanic	2.30	2.51
Water-soluble	0.0050	2.99
Soot	0.0118	2.000

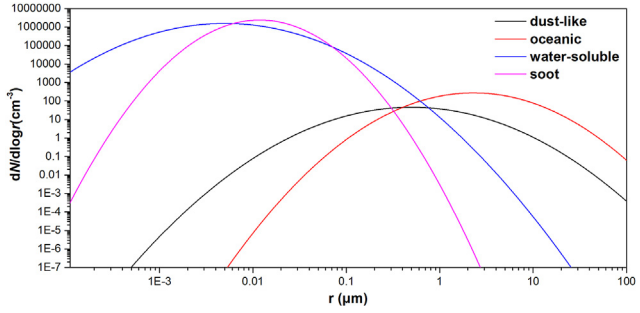

Figure 2. Lognormal particle size distributions of the four components.

$$V_j = \frac{4\pi}{3N_j}\int_0^{+\infty} r^3 \frac{dN_j(r)}{dr}dr, \tag{7}$$

where N_j is the particle number when the extinction coefficient at 0.55 μm is 1.0 km^{-1}. For the retrieved Lidar data, the extinction coefficient at 0.55 μm can hardly target the value of 1.0 km^{-1}. Thus, the normalization parameter A is introduced for the inversion of APSD which is shown in Eq. (8),

$$n(r) = A \cdot n_0(r), \tag{8}$$

where A is the normalization parameter, n is the modified APSD results, and n_0 is the original APSD. When observing the APSD with Lidar, the normalization parameter needs to be calibrated using another particle distribution measuring device. The normalization parameter can be regarded as a systematic parameter that can maintain a stable value for a period of time after the calibration of the Lidar system.

Table 2. V_j and N_j values for the four components.

Component	V_j (μm^3)	N_j (cm^{-3})
Dust-like	113.98352	54.73400
Oceanic	5.14441	276.0500010
Water-soluble	113.98352×10^{-6}	1.86850×10^6
Soot	59.777553×10^{-6}	1.805820×10^6

2.4. Calculation of extinction coefficients using Mie theory

The calculation of the extinction coefficients from the 6S particle distribution is another important step. Generally, the Mie theory is used to gain the optical coefficients and the Mie scattering theory is based on Maxwell's equations (Vermote et al., 1997). By analyzing and calculating the transmission and scattering field of the scattering particle and calculating the scattering, absorption, and extinction cross section, which reflect the total scattering, absorption, and extinction ability of the incident wave particle, the Mie theory can be used to obtain the exact solution for a spherical particle for the scattering and absorption of electromagnetic waves. The calculation of the optical parameters using Mie theory is essentially the calculation of the scattering, absorption, and extinction efficiency factors. And the calculation is made by Eqs. (9), (10), and (11).

$$Q_e(\alpha, m) = \frac{2}{\alpha^2}\sum_{n=1}^{\infty}(2n+1)\mathrm{Re}(a_n + b_n), \tag{9}$$

$$Q_s(\alpha, m) = \frac{2}{\alpha^2}\sum_{n=1}^{\infty}\left(2n+1\right)\left(|a_n|^2 + |b_n|^2\right), \tag{10}$$

$$Q_a(\alpha, m) = Q_e(\alpha, m) - Q_s(\alpha, m), \tag{11}$$

where m is the complex refractive index, α is the scaling parameter ($\alpha = 2\pi r/\lambda$), r is the particle radius, λ is the wavelength, and a_n and b_n are the amplitudes of the nth electric and nth magnetic parts of the charge of the particle, respectively. a_n and b_n are only related to α and m. These two parameters are calculated by Eqs. (12) and (13).

$$a_n = \frac{\psi_n'(y)\psi_n(x) - m\psi_n(y)\psi_n'(x)}{\psi_n'(y)\zeta_n(x) - m\psi_n(y)\zeta_n'(x)}, \tag{12}$$

$$b_n = \frac{m\psi_n'(y)\psi_n(x) - \psi_n(y)\psi_n'(x)}{m\psi_n'(y)\zeta_n(x) - \psi_n(y)\zeta_n'(x)}, \tag{13}$$

where x is the scaling parameter, that is, $x = \alpha = kr = \frac{2\pi r}{\lambda}$, and $y = mkr$. ψ_n and ζ_n are the Riccati-Bessel functions, which is shown in Eqs. (14), (15), and (16).

$$\psi_n(x) = (-1)^n x^{n+1}\frac{d^n}{(xdx)^n}\left(\frac{\sin x}{x}\right). \tag{14}$$

$$\chi_n(x) = (-1)^n x^{n+1}\frac{d^n}{(xdx)^n}\left(\frac{\cos x}{x}\right). \tag{15}$$

$$\zeta_n(x) = \psi_n(x) + i\chi_n(x). \tag{16}$$

When the particle size distribution value is n(r), the extinction coefficient σ_e, scattering coefficient σ_s, and absorption coefficient σ_a are determined using $Q_e(\alpha, m)$, $Q_s(\alpha, m)$, and $Q_a(\alpha, m)$, respectively. And the optical efficiency factors are calculated by Eq. (17).

$$\sigma_i = \pi \int_0^{\infty} Q_i(\alpha, m) n(r) r^2 dr, \ (\mathrm{I} = \mathrm{e}, \ \mathrm{s}, \ \mathrm{a}). \tag{17}$$

3. Method verification

To verify the reliability of the proposed method, particle size distribution was measured using a scanning mobility particle sizer (SMPS) placed on the roof of a building in the park. The particle number-size distribution in the range of 11.1–414.2 nm was measured at 1.5-min intervals using the SMPS, which included a differential mobility analyzer (TSI model 3081, USA) and a condensation particle counter (TSI model 3750, USA). The device was set up in Hefei City, China. The observations were conducted on November 19, 2020, and the weather was clear and dry. The original APSD data shown in Figures 3a and 3b are the extinction coefficients calculated from the Mie theory. The extinction results were used to retrieve APSD to make comparison with original data.

Figure 4 presents a comparison of the retrieved APSD data, which is matched at 0.0–0.4 μm and 0.15–0.4 μm. The results show that the APSD retrieved using the lognormal distribution method fits well with the original distribution data in the 0.15–0.4 μm range, and the retrieval process causes a significant deviation between the APSD results and original data when the retrieval wavelength expands to 0.0–0.4 μm. This phenomenon occurred in the retrieval process of every set of data, so it is concluded that the method is not suitable for particle sizes of less than 0.15 μm. As for Lidar observation, there is no signal wavelength of less than 0.15 μm, so the method is acceptable for Lidar data retrieval, and the effective range of the retrieved APSD should be in the range more than 0.15μm.

The observations were collected on land so the oceanic aerosol component was removed. To study the influences of the different component combinations on the retrieval of the APSD, the single-component, double-component, and three-component cases were calculated at 0.15–0.4 μm, and the results are shown in Figure 5. The results of the Pearson correlation analysis are presented in Table 3, and the analysis was conducted for APSD retrieval wavelengths of 0.0–0.4 μm and 0.15–0.4 μm. The terms dust-like, water-soluble, and soot are abbreviated as dl, ws, and st in Figure 5 and Table 3.

Three conclusions were drawn based on the results shown in Figure 5 and Table 3. First, the correlations of the APSDs at 0.15–0.4 μm are generally greater than those at 0.0–0.4 μm. This is consistent with the conclusion stated above. Second, the correlation results of the combinations containing the water-soluble component are much better than those that do not contain the water-soluble component, and their correlations are all greater than 0.95. The proportion of the water-soluble component remains high when retrieving the APSD using three-component combinations, but the proportion of soot is a hundred or even a thousand times lower. The large gap between these components shows that the water-soluble particles were dominant in the atmosphere

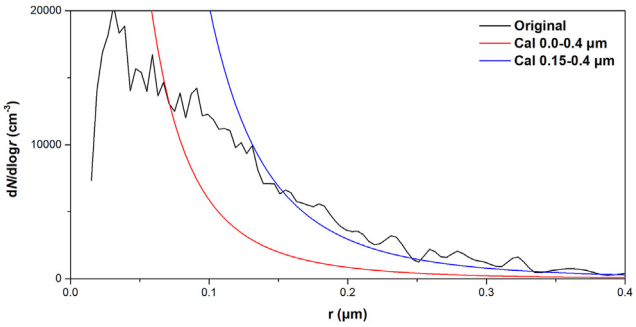

Figure 4. The retrieved APSD results in the matching wavelength ranges of 0.0–0.4 μm and 0.15–0.4 μm.

around the observation location and the soot particles were almost absent. This conclusion is consistent with the weather conditions and atmospheric situation during the data collection. Third, it can be revealed from the results of these three groups that, the atmosphere aerosol particle can be characterized just by a bimodal combination of lognormal functions which are the distribution of water-soluble and soot aerosol particles respectively. The similar phenomenon appears in another marine observation we are doing recently. The oceanic and water-soluble aerosols dominate the atmosphere above the sea level, and the Lidar-retrieved result which is combination of these two components fits well with the measured APSD data. It seems that a bimodal combination could be enough for some situations.

4. Application of the method

Using the lognormal distribution method, the Lidar observations acquired in March 2021 in Minqin County, Wuwei City, China, were retrieved to obtain the APSD. A sunphotometer (CE318) was using to obtain APSD and make a comparison with the Lidar data. Due to the lack of local particle size distribution data, a set of historical APSD data was selected as a reference to estimate the normalization parameter, and the value was determined to be 14.5 (Yu et al., 2017). The Lidar used an Nd:YAG laser with an emission wavelength of 0.532 μm, and the five receiving signal wavelengths were 0.28 μm, 0.295 μm, 0.532 μm, 0.56 μm, and 0.59 μm Figure 6 shows the extinction coefficients and APSD retrieved from the Lidar data at 03:20 am on March 11, 2021 and 03:20 am on March 14, respectively. It should be noted that when retrieving the ASPD of a certain vertical layer, the extinction coefficient data within the height range are averaged in the calculation.

According to the meteorological data, the weather was clear and dry, and the air quality was quite good on March 11, and the weather on March 14 was dusty. In addition, no clouds were observed by the Lidar during the acquisition period. Figures 6a and 6c show the extinction coefficient profile at 0.532 μm, and Figures 6b and 6d show retrieved APSDs at 200–500 m, 500–800 m, and 800–1000 m. The extinction

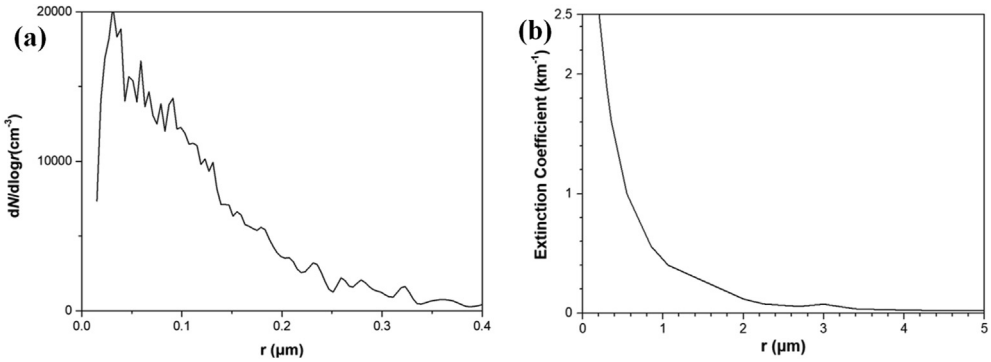

Figure 3. (a) The original APSD data, and (b) the extinction coefficients calculated from the Mie theory.

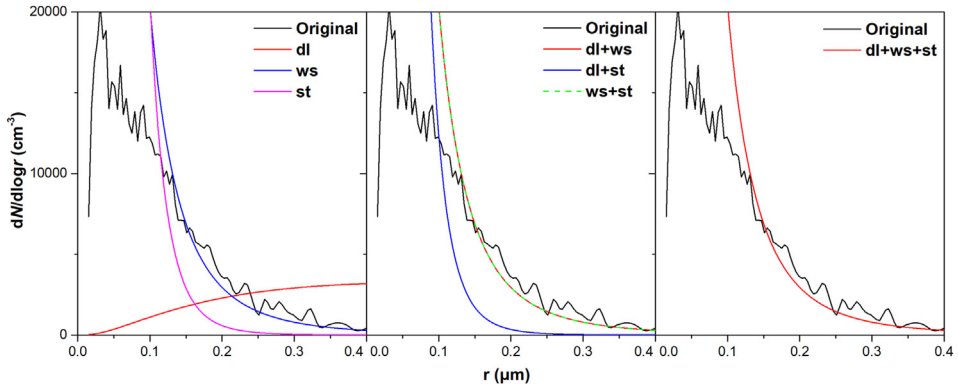

Figure 5. The retrieved APSD results with different component combinations: (a) Single-component, (b) Double-component, and (c) Three-component. All of the results were retrieved at 0.15–0.4 μm.

Table 3. Pearson correlation coefficients of the retrieved APSD and the original data.

Components	Corr coeff (0–0.4 μm)	Corr coeff (0.15–0.4 μm)
dl	-0.97104	-0.97635
ws	0.52662	0.97496
st	0.44348	0.90470
dl + ws	0.52662	0.97496
dl + st	0.43547	0.90469
ws + st	0.52474	0.97489
dl + ws + st	0.52566	0.97492

results on March 11 show that the near-ground atmosphere was very clean, and the near-ground extinction coefficients on March 14 were around 0.3–0.4 which was generally considered to be caused by dust particles (Groß et al., 2013). The APSD results show that the dusty APSD data were 50 times more than clean weather and the Lidar data have a strong response to dust weather. The APSDs in different vertical layers reveal that the dusty weather strongly influenced the atmosphere from the ground to 800 m height and caused a great increase of aerosol concentrations. Oppositely, the condition of atmosphere above 800 m is similar to the good weather on March 11, and there seems no influences from the dusty weather.

Figure 7 shows the APSDs retrieved by Lidar and CE318. Figure 7a was obtained on March 11 which was in good weather, and 7b was on March 14, a dusty day. The Pearson correlation coefficients are more than 0.95 on the clear day and are more than 0.90 on the dust day, respectively. It can be proved that the Lidar APSD results are strongly correlated with the CE318 results.

This experiment demonstrates that the APSD retrieval method based on the lognormal particle distribution and the 6S can be used to obtain APSD data in a certain vertical layer. The retrieved APSD results coincide well with the meteorological data and reflect the aerosol microphysical characteristics and atmospheric conditions at the observation location. In the next phase of the APSD retrieval method investigation, we will conduct the synchronous observation with Lidar and other APSD measuring device to carry out a more detailed study on the Lidar APSD inversion and the calculation of the normalization parameter, which could be a significant part in this method to improve the precision of

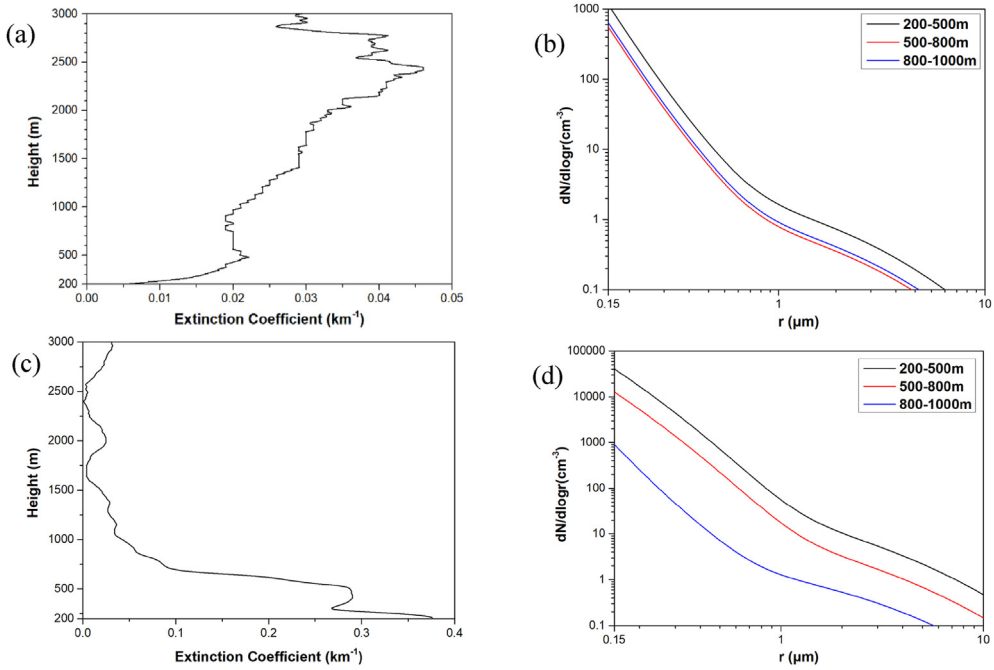

Figure 6. (a) (c) The extinction coefficient profile, and (b) (d) the APSDs of the different vertical layers. (a) and (b) were retrieved from the dataset obtained at 03:20 am on March 11, 2021. (a) and (b) were retrieved from the dataset obtained at 03:20 am on March 14, 2021.

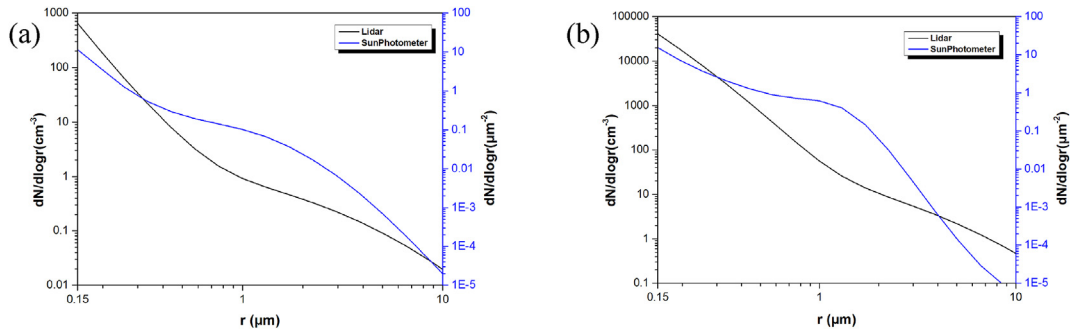

Figure 7. (a) APSDs retrieved by Lidar and CE318 on March 11, and (b) on March 14. The APSDs retrieved by Lidar are at 200–500 m.

inversion. Also, we expect to find out the dependency relationship between the values of normalization parameter and different meteorological conditions.

Declarations

Author contribution statement

Yuchen Shi: Performed the experiments; Wrote the paper.

Wenqing Liu: Conceived and designed the experiments.

Yunsheng Dong: Conceived and designed the experiments; Performed the experiments; Contributed reagents, materials, analysis tools or data.

Xuesong Zhao: Conceived and designed the experiments; Contributed reagents, materials, analysis tools or data.

Yan Xiang: Analyzed and interpreted the data; Contributed reagents, materials, analysis tools or data.

Tianshu Zhang: Contributed reagents, materials, analysis tools or data.

Lihui Lv: Analyzed and interpreted the data.

Funding statement

This work was supported by National Natural Science Foundation of China [41941011].

Data availability statement

The authors do not have permission to share data.

Declaration of interests statement

The authors declare no conflict of interest.

Additional information

No additional information is available for this paper.

Acknowledgements

Y. Shi and all of the other co-authors would like to thank the National Natural Science Foundation for support.

We thank LetPub (www.letpub.com) for its linguistic assistance during the preparation of this manuscript.

References

Di, H., Wang, Z., Hua, D., 2019. Precise size distribution measurement of aerosol particles and fog droplets in the open atmosphere. Opt Express 27, A890–A908.

Ding, Y., Li, Q., Liu, Y., Zhang, L., Song, Y., Zhang, J., 2009. Atmospheric aerosols, Air pollution and climate change. Meteorol. Mon. 35 (3), 3–14 (in Chinese).

Fernald, F.G., 1984. Analysis of atmospheric lidar observations: some comments. Appl. Opt. 23, 652–653.

U. NOAA, Force, U.A., 1976. US Standard Atmosphere.

Groß, S., Esselborn, B., Weinzierl, B., Wieth, M., Fix, A., Petzold, A., 2013. Aerosol classification by airborne high spectral resolution lidar observations. Atmos. Chem. Phys. 13 (5), 2487–2505.

Mao, J., Zhang, J., Wang, M., 2002. Summary comment on research of atmospheric aerosol in China. Acta Meteorol. Sin. 5, 625–634 (in Chinese).

Müller, D., Wandinger, U., Ansmann, A., 1999a. Microphysical particle parameters from extinction and backscatter lidar data by inversion with regularization: theory. Appl. Opt. 38, 2346–2357.

Müller, D., Wandinger, U., Ansmann, A., 1999b. Microphysical particle parameters from extinction and backscatter lidar data by inversion with regularization: simulation. Appl. Opt. 38, 2358–2368.

Müller, D., Wagner, F., Wandinger, U., Ansmann, A., Wendisch, M., Althausen, D., von Hoyningen-Huene, W., 2000. Microphysical particle parameters from extinction and backscatter lidar data by inversion with regularization: experiment. Appl. Opt. 39, 1879–1892.

Rao, Z., He, T., Hua, D., Chen, R., 2018. Remote sensing of particle mass concentration using multi-wavelength Lidar. Spectrosc. Spectr. Anal. 38 (4), 1025–1030 (in Chinese).

Tanre, D., Deroo, C., Dehaut, P., Herman, M., Morrcrette, J.J., Perbos, J., Deschamps, P.Y., 1986. Simulation of the Satellite Signal in the Solar Spectrum: User's Guide. LOA, Lille.

Vermote, E.F., Tanre, D., Deuze, J.L., Herman, M., Morcette, J., 1997. Second simulation of the satellite signal in the solar Spectrum, 6S: an overview. IEEE Trans. Geosci. Rem. Sens. 35 (3), 675–686.

Yan, D., Di, H., Zhao, J., Wen, X., Wang, Y., Song, Y., Hua, D., 2019. Improved algorithm of aerosol particle size distribution based on remote sensing data. Appl. Opt. 58, 8075–8082.

Yang, Z., Zhang, X., Che, H., Zhang, X., Hu, X., Zhang, L., 2008. An introductory study on the calibration of CE318 sunphotometer. J. Appl. Meteorol. Sci. 3, 297–306 (in Chinese).

Yu, Y., Zhao, S., Wang, B., Fu, P., He, J., 2017. Pollution characteristics revealed by size distribution properties of aerosol particles at urban and suburban sites, northwest China. Aerosol Air Qual. Res. 17, 1784–1797.